Communication: Nucleation of quantized vortex rings in 4He nanodroplets

David Mateo, Antonio Leal, Alberto Hernando, Manuel Barranco, Martí Pi, Fausto Cargnoni, Massimo Mella, Xiaohang Zhang, and Marcel Drabbels

Communication: Nucleation of quantized vortex rings in ⁴He nanodroplets

David Mateo,[1] Antonio Leal,[1] Alberto Hernando,[2] Manuel Barranco,[1] Martí Pi,[1] Fausto Cargnoni,[3] Massimo Mella,[4] Xiaohang Zhang,[5] and Marcel Drabbels[5]

[1]*Departament ECM, Facultat de Física, and IN[2]UB, Universitat de Barcelona, Diagonal 645, 08028 Barcelona, Spain*
[2]*Laboratory of Theoretical Physical Chemistry, Institut des Sciences et Ingénierie Chimiques, Swiss Federal Institute of Technology Lausanne (EPFL), CH-1015 Lausanne, Switzerland*
[3]*Istituto di Scienze e Tecnologie Molecolari (ISTM), Consiglio Nazionale delle Ricerche, via Golgi 19, 20133 Milano, Italy*
[4]*Dipartimento di Scienza ed Alta Tecnologia, Università degli Studi dell'Insubria, via Valleggio 11, 22100 Como, Italy*
[5]*Laboratoire de Chimie Physique Moléculaire, Swiss Federal Institute of Technology Lausanne (EPFL), CH-1015 Lausanne, Switzerland*

Whereas most of the phenomena associated with superfluidity have been observed in finite-size helium systems, the nucleation of quantized vortices has proven elusive. Here we show using time-dependent density functional simulations that the solvation of a Ba^+ ion created by photoionization of neutral Ba at the surface of a ⁴He nanodroplet leads to the nucleation of a quantized ring vortex. The vortex is nucleated on a 10 ps timescale at the equator of a solid-like solvation structure that forms around the Ba^+ ion. The process is expected to be quite general and very efficient under standard experimental conditions. © *2014 AIP Publishing LLC.* [http://dx.doi.org/10.1063/1.4870245]

Helium clusters are paradigms of finite-size quantum systems.[1] These nanodroplets attain a temperature of 0.37 K,[2,3] clearly below the superfluid transition temperature of liquid ⁴He, T_λ= 2.17 K. Quantum Monte Carlo calculations have revealed that even very small droplets containing less than 100 helium atoms display features pertaining to the superfluid state of bulk liquid helium.[4–6] Although such small systems are expected to be superfluid, it is not obvious whether phenomena generally associated with superfluidity in bulk helium will be manifested in these nanosystems. First indications of a vanishing viscocity were provided by spectroscopic experiments on helium droplets doped with carbonyl sulfide (OCS). The IR spectrum of OCS revealed a well resolved rovibrational structure, which has been taken as evidence that the OCS molecule can freely rotate inside the ⁴He droplet.[7] The minimum number of ⁴He atoms required to produce the effect was about 60, in good agreement with the calculations.[4] However, recent experiments indicate that the system is more complex than initially anticipated as the temporal evolution of rotational wave packets cannot be explained with the free rotation of the embedded molecule.[8] Another subtle manifestation of superfluidity is the frictionless displacement of impurities inside helium if they move at velocities below the so-called Landau velocity. Recent experiments in which impurities were accelerated out of helium droplets by means of electronic excitation have revealed that a critical Landau velocity exists even for droplets consisting of less than one thousand helium atoms.[9,10]

In the quest for manifestations of superfluidity in nanoscale helium droplets, the nucleation of quantized vortices has proven elusive for years. Only recently indications have been found for the presence of vortices in large helium droplets.[11] These droplets consisting of $10^7 - 10^{10}$ atoms

were produced by fragmentation of a cryogenic fluid. Such large droplets are true mesoscopic pieces of superfluid helium, having radii in the range of $50 - 500$ nm. It is thus somewhat expected that they may host vortex lines, either pre-existing in the fluid or created in the fragmentation process. The main question is whether vortices may also be nucleated in much smaller droplets consisting of only a few hundreds or thousands of helium atoms. These droplets are expected to carry enough energy and angular momentum to create a vortex which is especially robust due to the lack of decay channels that conserve both energy and angular momentum.[12] Moreover, in experiments with doped droplets, the pickup of impurities might lead to vortex nucleation. Once nucleated, they are stabilized by pinning to the impurity inside the droplet.[13] One limitation of all these theoretical studies is that they take for granted that vortices have been nucleated.

Vortex ring nucleation around electron bubbles in superfluid helium has recently been addressed using density functional (DF) simulations of different complexity.[14–16] The nucleation of vortices by cations or neutral impurities, which have very different helium solvation structures than electrons, has not been addressed by realistic methods, only by approximate methods that model these impurities as repulsive rigid spheres.[17] A full dynamical description of the process for these systems is thus still lacking.[18,19] In the present work, we show using a time-dependent DF approach that the dynamics following the photoionization of neutral Ba atoms located on the surface of helium nanodroplets leads to vortex nucleation.

At variance with other possible methods for vortex nucleation, the current process is initiated using a well-defined, experimentally reproducible condition, i.e., the equilibrium configuration of Ba atom located at a surface dimple. Hence,
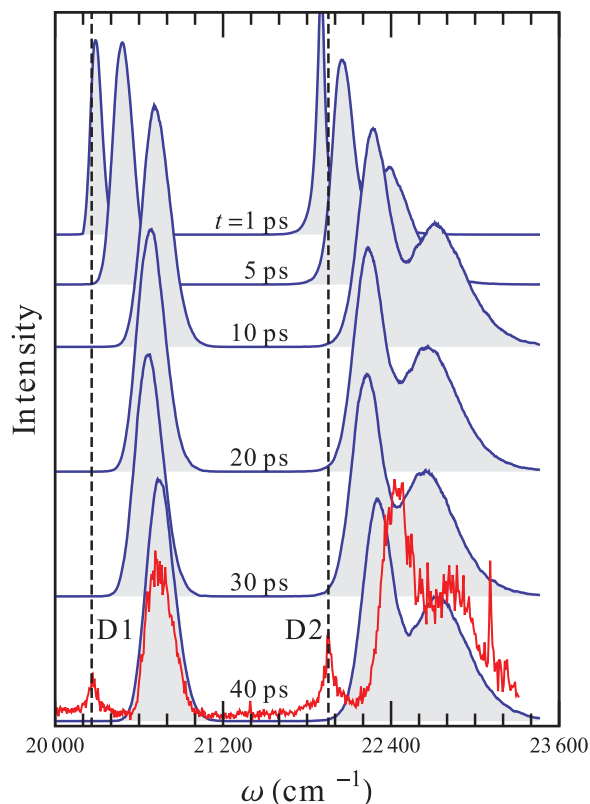
FIG. 1. Time-resolved absorption spectrum of Ba^+ in a $^4He_{1000}$ droplet. The experimental spectrum for helium droplets consisting on average of 2700 atoms is shown in red. The vertical lines indicate the D1 and D2 transitions of the free Ba^+ cation.

FIG. 2. Snapshots of the temporal evolution of the $Ba@^+He_{1000}$ system after photoionization of the neutral Ba atom located at the droplet surface. Panels 1 to 6 correspond to the helium densities at times $t = 0, 8, 14, 47, 60,$ and 220 ps. (Multimedia view) [URL: http://dx.doi.org/10.1063/1.4870245.1]

vortex nucleation is expected to be highly efficient in these types of experiments.

Recent experiments on the solvation dynamics of Ba^+ created at the surface of small helium nanodroplets serve as reference for the present calculations.[20] The $6p \leftarrow 6s$ transition of Ba^+ shown in Fig. 1 was found to coincide with that of Ba^+ in bulk superfluid helium, indicating that the Ba^+ ion becomes fully solvated by the helium on the nanosecond timescale of the experiment.

We describe the solvation process of the Ba^+ ion by a three dimensional time-dependent DF approach in which the superfluid is described by a complex effective wavefunction $\Psi_{He}(\mathbf{r}, t)$ such that $\rho(\mathbf{r}, t) = |\Psi_{He}(\mathbf{r}, t)|^2$ and the Ba^+ impurity, due to its large mass, is treated as a classical particle with position $\mathbf{r}_{Ba^+}(t)$.[10] To obtain the dynamical evolution of the $Ba^+@^4He_{1000}$ system, the following coupled 3D time-dependent equations have been solved:

$$i\hbar \frac{\partial}{\partial t} \Psi_{He} = \left[-\frac{\hbar^2}{2m_{He}} \nabla^2 + \frac{\delta \mathcal{E}_{He}}{\delta \rho(\mathbf{r})} + V_{6s}^+(\mathbf{r} - \mathbf{r}_{Ba^+}) \right] \Psi_{He}$$

$$m_{Ba^+} \ddot{\mathbf{r}}_{Ba^+} = -\nabla_{\mathbf{r}_{Ba^+}} \left[\int d\mathbf{r} \rho(\mathbf{r}) V_{6s}^+(\mathbf{r} - \mathbf{r}_{Ba^+}) \right],$$

(1)

where $\mathcal{E}_{He}$ is the DF potential energy density per unit volume and $V_{6s}^+(\mathbf{r} - \mathbf{r}_{Ba^+})$ is the ground state Ba^+-He pair potential. To avoid reflections at the boundaries of the calculation cell, an absorption potential has been added to the Hamiltonian.[21] The DF used in the present work[22] is a modified version of
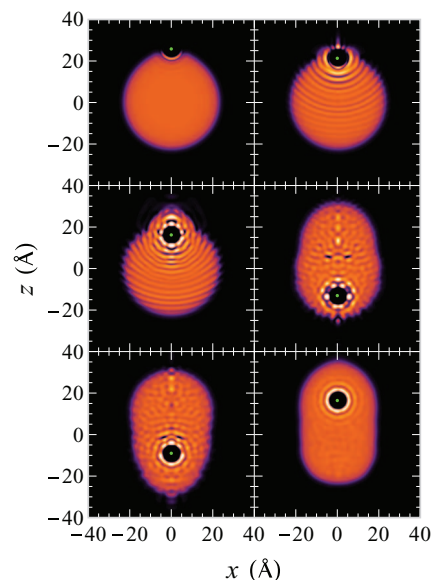
the Orsay-Trento DF[23] able to handle very structured helium configurations as those expected to appear around very attractive impurities such as cations. This functional has been found to accurately reproduce the helium configurations calculated by Quantum Monte Carlo methods.[24,25] Details of how the above equations have been solved can be found in Refs. 10, 21, and 26. The modelling of the solvation process critically depends on the quality of the ingredients entering the calculation. In the absence of accurate He-Ba^+ pair potentials, these have been computed in this study at the CCSD(T) level of theory. The 46 core electrons of Ba^+ are described by the Def2 pseudopotential,[27] while for the outermost 9 electrons the QZVP quadruple-z set is used.[28] The He atom has been assigned the aug-cc-pV5Z basis,[29] and a 3s3p2d set of bond functions has been located at midway between the two nuclei.[30]

The initial conditions for solving the equations correspond to those at the time of ionization, i.e., the equilibrium configuration of the neutral $Ba@4He_{1000}$ complex. DF calculations find this configuration to have the Ba atom residing in a dimple at the surface of the droplet,[31] in agreement with experiments.[32,33] Snapshots of the dynamical evolution of the $Ba^+@4He_{1000}$ system are presented in Fig. 2 (Multimedia view). During the initial phase of the solvation process, supersonic density waves are emitted into the droplet. Similar density waves have been observed when alkali atoms located at the surface of the droplets are excited and have been analyzed in detail.[34] Due to the attractive interaction of the Ba^+ with the helium, the ion moves towards the center of the droplet. After approximately 8 ps, the barium ion is fully surrounded by the helium and a few picoseconds later a solid-like solvation layer with localized helium atoms dubbed "snowball" forms. As the Ba^+ is accelerated further towards the center of the droplet, it interacts with the helium density waves reflected from the droplet surface, leading to fast
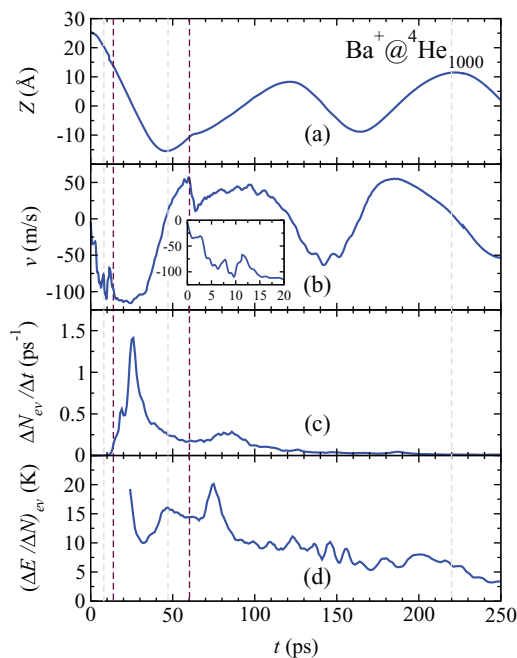
FIG. 3. Position (a) and velocity (b) of the Ba^+ ion with respect to the helium droplet center-of-mass. The inset shows the velocity of Ba^+ during the first 20 ps. Number of evaporated helium atoms per unit time (ps^{-1}) (c) and energy (K) removed from the helium droplet per evaporated helium atom (d). The vertical dashed lines indicate the times corresponding to the snapshots 2 to 6 shown in Fig. 2, where the dark lines correspond to times just after vortex nucleation and just before vortex annihilation.

structural changes in the solvation structure, see Fig. 2 (Multimedia view). After passing the center of the droplet at $t \approx 20$ ps, the ion is decelerated and subsequently reflected at the droplet surface at $t \approx 40$ ps. Figure 3 shows the motion of the Ba^+ ion with respect of the $^4He_{1000}$ center of mass in terms of position and velocity as a function of time. The Ba^+ continues oscillating back and forth in the droplet with a period of ~ 100 ps up to the end of the simulation, i.e., 350 ps. During this period, the helium density waves damp out and the fluctuating solvation structure surrounding the ion becomes homogenous, see Fig. 2 (Multimedia view), in agreement with the calculated equilibrium structure of the $Ba^+@^4He_{1000}$ system. After the first oscillation, during which the velocity of the Ba^+ changes erratically due to interaction with the helium density waves, the velocity of the Ba^+ remains at all times below the critical Landau velocity, which has been found to be 96 m/s for the DF used in this work.[22] Consequently, the Ba^+ is expected to keep oscillating for much longer times than the 350 ps simulation, as translational energy can only be removed by the interaction with droplet surface oscillations and deformations.

The solvation of the ion is reflected in the $6p \leftarrow 6s$ absorption spectrum of Ba^+. The time resolved spectrum has been obtained by the DF sampling method described in Ref. 35. The 6p excited state He-Ba^+ pair potentials required for the calculations have been computed using the CI method including single and double excitations (CISD), and using the same pseudopotential and basis sets adopted for the ground state. The spectrum shown in Fig. 1 reveals an obvious evolution with time that could be quantitatively checked by time-
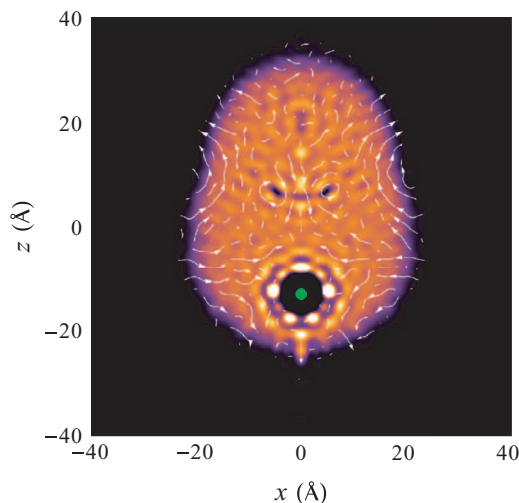

FIG. 4. Snapshot of the helium density at 45 ps showing the snowball and a quantized vortex ring. The circulation lines are represented in white.

resolved absorption experiments. At $t = 1$ ps, the spectrum is red-shifted with respect to the corresponding gas phase transitions, reflecting the non-equilibrium helium density distribution surrounding the Ba^+ at the start of the evolution. During the first 10 ps, as the helium rearranges to solvate the Ba^+ ion, the spectrum shifts towards the blue, and a good agreement with the experimental spectrum is observed. From 10 ps onwards, the spectrum displays a small variation with time reflecting the change in the helium environment as the Ba^+ traverses the droplet.

The solvation of the Ba^+ releases energy into the helium droplet as a result of which helium atoms desorb from the droplet during the evolution of the system. By monitoring the number of atoms leaving the simulation box we find that most of the atoms desorb from the droplet during the first 100 ps at well-defined times, see Fig. 3. The atoms desorbing after 20 ps result from the formation of the solvation layer around the Ba^+ and leave the droplet in the backward direction, defined as the direction opposite to the initial acceleration of the Ba^+. The peak at 80 ps is related to the reflection of the Ba^+ at the droplet surface which leads to a large deformation of the droplet and the desorption of helium atoms in the forward direction. Since the desorption of these atoms is governed by dynamical processes, the amount of energy removed from the droplet by an atom, ≈ 20 K, is substantially larger than its binding energy of ≈ 6 K. At longer times the energy appears to be dissipated by an evaporative-like process.

Besides the dynamic formation of the Ba^+ snowball and the time-resolved absorption spectrum of this cation, the most interesting outcome of the calculations is the formation of a vortex ring at the equator of the Ba^+ solvation structure after about 13 ps, see Fig. 2 (Multimedia view). This vortex ring slips around the ion and eventually detaches from it at 24 ps. The cross section of this vortex ring is readily recognized as the two dark spots behind the ion bubble in the helium density at $t = 45$ ps presented in Fig. 4. Superimposed on the helium density displayed in this figures are the circulation lines. These clearly reveal a circular flow field around the vortex. Calculation of the circulation around the core yields

a value of unity in units of h/m_{He}, indicating that this vortex ring is quantized. The nucleation of the vortex is reflected in the translational motion of the Ba$^+$. As can be seen in Fig. 3, the nucleation of the vortex temporarily decelerates the ion bubble, that then accelerates anew when the vortex detaches. Using this velocity change, the vortex energy can be estimated to be on the order of 60 K. This value can be compared to the vortex energy, E_{ring}, calculated using the expression:[19,36]

$$E_{ring} = \frac{2\pi^2\hbar^2}{m_{He}}\rho_0 R\left(\ln\frac{8R}{a} - 1.615\right), \qquad (2)$$

with a the vortex core size, R the vortex radius and ρ_0 the helium number density at large distance. Taking the values for the present system, $a = 0.7$ Å, $R = 4.2$ Å, and $\rho_0 = 0.0218$ Å^{-3} corresponding to the number density of a pure helium droplet, we obtain an energy of $\sim$46 K. This compares fairly well with the value determined from the velocity change of the Ba$^+$, considering that Eq. (2) is only valid in the limit of $R \gg a$. After detachment, the vortex ring moves with a nearly constant speed of 50 m/s as determined from the displacement of the vortex core in the time interval $t = 30 - 50$ ps. This value is slightly less than the self-induced speed of $v_{ring} = 61$ m/s for a vortex with the aforementioned characteristics, as calculated from:[19,36]

$$v_{ring} = \frac{\hbar}{2\,m_{He}R}\left(\ln\frac{8R}{a} - 0.615\right). \qquad (3)$$

The vortex ring is eventually annihilated at 61 ps when it collides with the Ba$^+$ that has been reflected at the droplet surface. The annihilation of the vortex ring leads to a strong reduction of the Ba$^+$ speed, as is clearly visible in Fig. 3. At the same time helium density waves emerge from the solvation structure surrounding the Ba$^+$ ion. These waves carry away most of the energy released by the annihilation of the vortex.

The present results indicate that quantized vortex rings are efficiently created in helium droplets by the solvation of a Ba$^+$ ion. From the calculations it becomes clear that vortex nucleation is a local process, see Fig. 2 (Multimedia view). Most likely the large structural changes in the liquid close to the attractive impurity are responsible for the high efficiency of the process. We therefore expect vortex nucleation to be largely independent of droplet size and impurity. As alkali atoms, like the heavy alkaline-earth atoms, are located at the droplet surface and have strongly attractive ion-helium interaction potentials they should behave very similar to barium. In particular, Na and Rb located at the surface of ^{4}He droplets are known to become solvated after ionization.[37,38] In view of the local character of the process, it is quite likely that ring vortices are also nucleated in helium droplets by the pickup of atoms or molecules having strong attractive interactions with the helium. We therefore conclude that, irrespective of their detection, the formation of vortex rings in doped droplets could be a much more common phenomenon than expected.

[1] J. P. Toennies and A. F. Vilesov, Angew. Chem., Int. Ed. **43**, 2622 (2004).

[2] D. M. Brink and S. Stringari, Z. Phys. D **15**, 257 (1990).

[3] M. Hartmann, R. E. Miller, J. P. Toennies, and A. Vilesov, Phys. Rev. Lett. **75**, 1566 (1995).

[4] P. Sindzingre, M. L. Klein, and D. M. Ceperley, Phys. Rev. Lett. **63**, 1601 (1989).

[5] M. V. Rama Krishna and K. B. Whaley, Phys. Rev. Lett. **64**, 1126 (1990).

[6] S. A. Chin and E. Krotscheck, Phys. Rev. B **45**, 852 (1992).

[7] S. Grebenev, J. P. Toennies, and A. Vilesov, Science **279**, 2083 (1998).

[8] D. Pentlehner, J. H. Nielsen, A. Slenczka, K. Molmer, and H. Stapelfeldt, Phys. Rev. Lett. **110**, 093002 (2013).

[9] N. B. Brauer, S. Smolarek, E. Loginov, D. Mateo, A. Hernando, M. Pi, M. Barranco, W. J. Buma, and M. Drabbels, Phys. Rev. Lett. **111**, 153002 (2013).

[10] D. Mateo, A. Hernando, M. Barranco, E. Loginov, M. Drabbels, and M. Pi, Phys. Chem. Chem. Phys. **15**, 18388 (2013).

[11] L. F. Gomez, E. Loginov, and A. Vilesov, Phys. Rev. Lett. **108**, 155302 (2012).

[12] K. K. Lehmann and R. Schmied, Phys. Rev. B **68**, 224520 (2003).

[13] F. Dalfovo, R. Mayol, M. Pi, and M. Barranco, Phys. Rev. Lett. **85**, 1028 (2000).

[14] D. Jin and H. J. Maris, J. Low Temp. Phys. **158**, 317 (2010).

[15] D. F. Jin and W. Guo, Phys. Rev. B: Condens. Matter **82**, 094524 (2010).

[16] F. Ancilotto, M. Barranco, and M. Pi, Phys. Rev. B: Condens. Matter **82**, 014517 (2010).

[17] N. G. Berloff, Phys. Lett. A **277**, 240 (2000).

[18] C. M. Muirhead, W. F. Vinen, and R. J. Donnelly, Philos. Trans. R. Soc. London, Ser. A **311**, 433 (1984).

[19] R. J. Donnelly, *Quantized Vortices in Helium II*, Cambridge Studies in Low Temperature Physics (Cambridge University Press, Cambridge, 1991), Vol. 3.

[20] X. Zhang and M. Drabbels, J. Chem. Phys. **137**, 051102 (2012).

[21] D. Mateo, D. Jin, M. Barranco, and M. Pi, J. Chem. Phys. **134**, 044507 (2011).

[22] F. Ancilotto, M. Barranco, F. Caupin, R. Mayol, and M. Pi, Phys. Rev. B **72**, 214522 (2005).

[23] F. Dalfovo, A. Lastri, L. Pricaupenko, S. Stringari, and J. Treiner, Phys. Rev. B **52**, 1193 (1995).

[24] F. Ancilotto, M. Pi, R. Mayol, M. Barranco, and K. K. Lehmann, J. Phys. Chem. A **111**, 12695 (2007).

[25] S. L. Fiedler, D. Mateo, T. Aleksanyan, and J. Eloranta, Phys. Rev. B **86**, 144522 (2012).

[26] A. Hernando, M. Barranco, R. Mayol, M. Pi, and M. Krośnicki, Phys. Rev. B **77**, 024513 (2008).

[27] M. Kaupp, P. V. Schleyer, H. Stoll, and H. Preuss, J. Chem. Phys. **94**, 1360 (1991).

[28] F. Weigend and A. Baldes, J. Chem. Phys. **133**, 174102 (2010).

[29] D. E. Woon and T. H. Dunning, Jr., J. Chem. Phys. **100**, 2975 (1994).

[30] F.-M. Tao, Z. Li, and Y.-K. Pan, Chem. Phys. Lett. **255**, 179 (1996).

[31] A. Hernando, R. Mayol, M. Pi, M. Barranco, F. Ancilotto, O. Bünermann, and F. Stienkemeier, J. Phys. Chem. A **111**, 7303 (2007).

[32] F. Stienkemeier, F. Meier, and H. O. Lutz, Eur. Phys. J. D **9**, 313 (1999).

[33] E. Loginov and M. Drabbels, J. Chem. Phys. **136**, 154302 (2012).

[34] A. Hernando, M. Barranco, M. Pi, E. Loginov, M. Langlet, and M. Drabbels, Phys. Chem. Chem. Phys. **14**, 3996 (2012).

[35] D. Mateo, A. Hernando, M. Barranco, R. Mayol, and M. Pi, Phys. Rev. B **83**, 174505 (2011).

[36] P. H. Roberts and J. Grant, J. Phys. A **4**, 55 (1971).

[37] E. Loginov and M. Drabbels, Phys. Rev. Lett. **106**, 083401 (2011).

[38] M. Theisen, F. Lackner, and W. E. Ernst, Phys. Chem. Chem. Phys. **12**, 14861 (2010).